EVOLUTIONARY BIOLOGY

Cassowary gloss and a novel form of structural color in birds

Chad M. Eliason[1,2]* and Julia A. Clarke[2]*

One of the two lineages of extant birds resulting from its deepest split, Palaeognathae, has been reported not to exhibit structural coloration in feathers, affecting inferences of ancestral coloration mechanisms in extant birds. Structural coloration in facial skin and eggshells has been shown in this lineage, but has not been reported in feathers. We present the first evidence for two distinct mechanisms of structural color in palaeognath feathers. One extinct volant clade, Lithornithidae, shows evidence of elongate melanin-containing organelles uniquely associated with glossy/iridescent color, a structural color mechanism found in fossil outgroups and neognath birds. We also demonstrate a structural basis for the exceptional gloss in extant cassowary feathers. We propose gloss as an intermediate phenotype between matte and iridescent plumage, conferred by a thick and smooth feather rachis. Rachis-based structural color has not been previously investigated. The new data illuminate the relationships between avian melanin-based coloration and feather structure.

INTRODUCTION

Birds produce structural colors in their skin and feathers using diverse mechanisms (*1*). Structural colors described in extant taxa—ranging from noniridescent blues to glossy blacks and an array of iridescent colors—are known in the branching structures of feathers, including barbs and barbules. Most shiny black birds create gloss, a form of structural coloration, with thin keratin layers and organized melanosomes in feather barbules (*2*), the same mechanism that generates thin-film iridescent colors (*1*). Shiny red birds create gloss with a flattened barb ramus (*3*). Noniridescent blue colors in feathers are generated with air bubbles in keratin inside feather barbs (*1*). Penguins also create blue structural color in their feather barbs with keratin nanofibers and changes in keratin organization (*4*, *5*), while blue skin in birds is generated by collagen nanofibers (*6*). Fossil evidence of structural color in feathers is present by the Late Jurassic in the repertoire of basal paravian dinosaurs (*7*) and is consistent with the structural coloration mechanisms known in extant bird barbs and barbules but not in the central rachis of the feather.

Integumentary structural coloration is well known in Neognathae, the clade including chickens, ducks, and songbirds (*8*), but, comparatively, little work has investigated the bases for colors observed in its sister clade, Palaeognathae [although see (*9*)]. Cassowaries and closely related emus are known to produce blue structural color in the facial skin (*6*). This color arises from coherent scattering by organized arrays of collagen fibers, similar to the arrays seen in neognaths (*6*). The closely related tinamous also produce iridescent structural colors in their eggshells with a thin, specialized cuticle layer (*10*). However, structural color in feathers has never been reported in palaeognaths and has been considered absent (*8*). Understanding whether and how structural colors are produced in the basally divergent Palaeognathae clade is important for inferences of ancestral states in crown birds and reconstructions of extinct dinosaur coloration.

Adult cassowaries have been described as having "silky" plumage as early as 1900s (*11*), with a reduced proportion of feather barbules along with widely spaced body contour feathers (*12*). However, evidence for a distinctive gloss, or "silkiness," relative to the feathers of closely related palaeognaths (e.g., emu and ostrich) and its potential morphological basis have never been investigated. Cassowaries have several feather modifications, including narrow feather vanes, loss of barbules, and thick feather rachises. Similar morphological "syndromes" have also been described in species with iridescent colors generated by modified feather barbules and organized melanosomes (*13*). Here, we evaluate evidence for, and the physical mechanism behind, gloss production in cassowary feathers, asking whether the acquisition of associated feather morphologies or "syndromes" copresent with gloss preceded its evolution. New morphological data and paleocolor predictions for a fossil palaeognath lineage, Lithornithidae, inform these assessments and enhance our understanding of the evolution of structural color mechanisms in Aves.

RESULTS

Quantifying glossiness from reflectance spectra

To quantify feather gloss, we measured both specular and diffuse reflectance across the bird-visible spectrum (300 to 700 nm; fig. S1) and determined gloss as the average ratio of specular to diffuse reflectance. The relationship (slope) between diffuse and specular reflectance was not significantly different in cassowaries and emus relative to other palaeognaths ($P = 0.088$; fig. S2). Gloss was exceptionally high in cassowaries and emus relative to other palaeognaths (fig. S3) and rivals that of some of the shiniest known birds (fig. S4).

Feather morphology and a new gloss mechanism in cassowaries

To understand the morphological basis of gloss, we imaged the surface of feathers using both atomic force microscopy (AFM) and transmission electron microscopy (TEM). AFM images showed that cassowary feathers are not appreciably smoother than control species, either in barbs or rachises (Table 1 and fig. S5). This finding mirrors previous results that showed no significant differences in barbule smoothness between glossy and matte feathers (*2*). Compared to

[1]Grainger Bioinformatics Center, Field Museum of Natural History, Chicago, IL, USA. [2]Jackson School of Geosciences and Integrative Biology, University of Texas at Austin, Austin, TX, USA.
*Corresponding author. Email: celiason@fieldmuseum.org (C.M.E.); julia_clarke@jsg.utexas.edu (J.A.C.)

other biomaterials, cassowary rachises are smoother than matte chicken eggshells (*10*) and mammalian hairs (*14*) but rougher than glossy tinamou eggshells (*10*). TEM images further showed no evidence for a thin film of keratin overlying melanosomes in the rachis, shown to be previously linked to glossiness in feather barbules (*2*). Lack of clear morphological nanoscale features led us to consider microscale traits that might influence how feathers are arranged on a bird's body. To do this, we used light microscopy to quantify aspects of feather microstructure that vary between glossy and matte species. Feather morphology differs greatly among ratites (*9*). Cassowaries, in particular, have bare feather barbs and rachises (i.e., lacking barbules) at the tips of feathers (fig. S6), along with thickened rachises (fig. S7) and narrow feather vanes (Fig. 1A).

Proximate basis of gloss

To further understand what morphological traits are associated with feather gloss, we used phylogenetic linear mixed models (PLMMs) that account for within-species measurements and phylogenetic signal in the relationship between variables. These analyses revealed that diffuse reflectance increased significantly with melanosome aspect ratio in palaeognaths ($\beta = -0.99$, $P_{MCMC} = 0.0089$; fig. S8A and table S1). Specular reflectance was significantly higher in species lacking feather barbules ($\beta = 19.0\%$, $P_{MCMC} = 0.011$; fig. S8B and table S1). Rachis width increased significantly with body size ($P_{MCMC} = 0.0013$), while feather vane width did not ($P_{MCMC} = 0.082$; see fig. S9). Ancestral state reconstructions show that palaeognaths likely had barbules along the full length of the feather, with cassowaries and emus later losing them (fig. S6).

Table 1. Surface roughness values measured from AFM images. Roughness [root mean square (RMS) values] measured with Gwyddion v. 2.50 for the rachis and barb ramus of three species. Lower RMS values indicate smoother surfaces.

Species	RMS surface roughness (nm)	
	Rachis	Barb ramus
Gray tinamou (*Tinamus tao*)	152.2	234.0
Common ostrich (*Struthio camelus*)	106.2	104.2
Southern cassowary (*Casuarius casuarius*)	99.0	103.4

Color in an extinct palaeognath

To further understand color evolution in palaeognaths, we examined melanosome morphologies in two extinct lithornithid specimens from the Early Eocene Green River Formation (*15*) using scanning electron microscopy (SEM). To predict coloration from SEM our image measurements, we used quadratic discriminant function analysis trained with two published datasets on melanosome morphologies in crown birds and nonavian dinosaur taxa (*7*, *16*). Some body regions of the extinct lithornithid *Calxavis grandei* were predicted as glossy black or weakly iridescent (Table 2). Lithornithid specimen AMNH FARB (American Museum of Natural History/Fossil Amphibians, Reptiles, and Birds) 30560 was predicted as having black wing coverts and glossy black or weakly iridescent primaries, and specimen AMNH FARB 30578 was predicted as glossy black with high (>89%) confidence on the tail and wing (Fig. 2 and Table 2). Results were qualitatively similar using a recent dataset including additional iridescent species (*16*).

DISCUSSION

While palaeognaths have been described as lacking structurally colored feathers, cassowaries show some of the highest values of gloss—a form of structural color—in studied birds (fig. S3). However, the mechanism by which this black gloss is achieved differs markedly

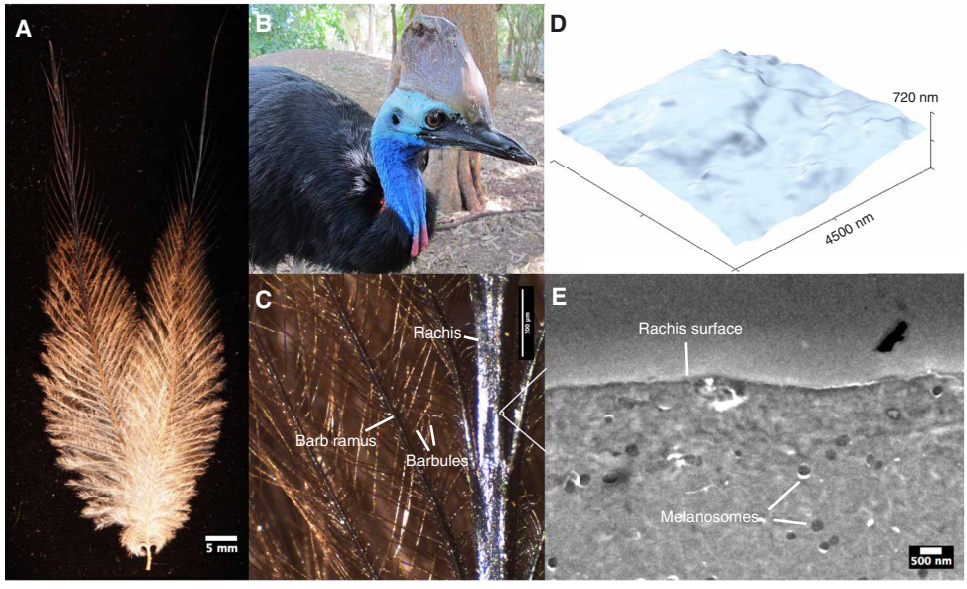

Fig. 1. Structural gloss in cassowary feathers. (**A**) Cassowary contour feather sampled from the upper left breast region. (**B**) Image of a southern cassowary (*C. casuarius*; photo credit: Albert Straub, CC license). (**C**) Close-up of feather from (A) showing microstructure. (**D**) AFM image of the surface of the rachis. (**E**) TEM image of the rachis. Scale bars, 5 mm (A), 500 μm (C), and 500 nm (E).

Table 2. Predicting color in extinct lithornithids. Discriminant function analysis results based on fossil melanosome morphology compared to a large dataset of extant birds (*7*). Cross-validation accuracy was 82%, and self-test accuracy was 77% [see (*23*) for details]. Note that probabilities calculated with the Nordén *et al.* (*16*) dataset only included melanosome length, width, length coefficient of variation (CV) and aspect ratio (AR), as other variables were not calculated in that study. All feather identities are tentative given the disarticulated nature of the fossil specimens.

Specimen	Sample no. (feather identity)	*N*	Length (nm)	Width (nm)	AR	Length CV	Width CV	AR skew	Class	Prob. Hu *et al.* (*7*)	Prob. Nordén *et al.* (*16*)
AMNH FARB 30560	4 (primaries)	59	763	195	4.0	2.58	2.97	0.71	Glossy	48%	58%
AMNH FARB 30560	5 (primaries or primary coverts)	113	943	272	3.6	1.74	1.88	0.71	Black	79%	71%
AMNH FARB 30578	7 (tail)	10	938	204	4.7	5.19	5.95	1.20	Glossy	96%	63%
AMNH FARB 30578	8 (crown)	19	949	196	5.0	4.64	3.30	0.30	Glossy	87%	87%

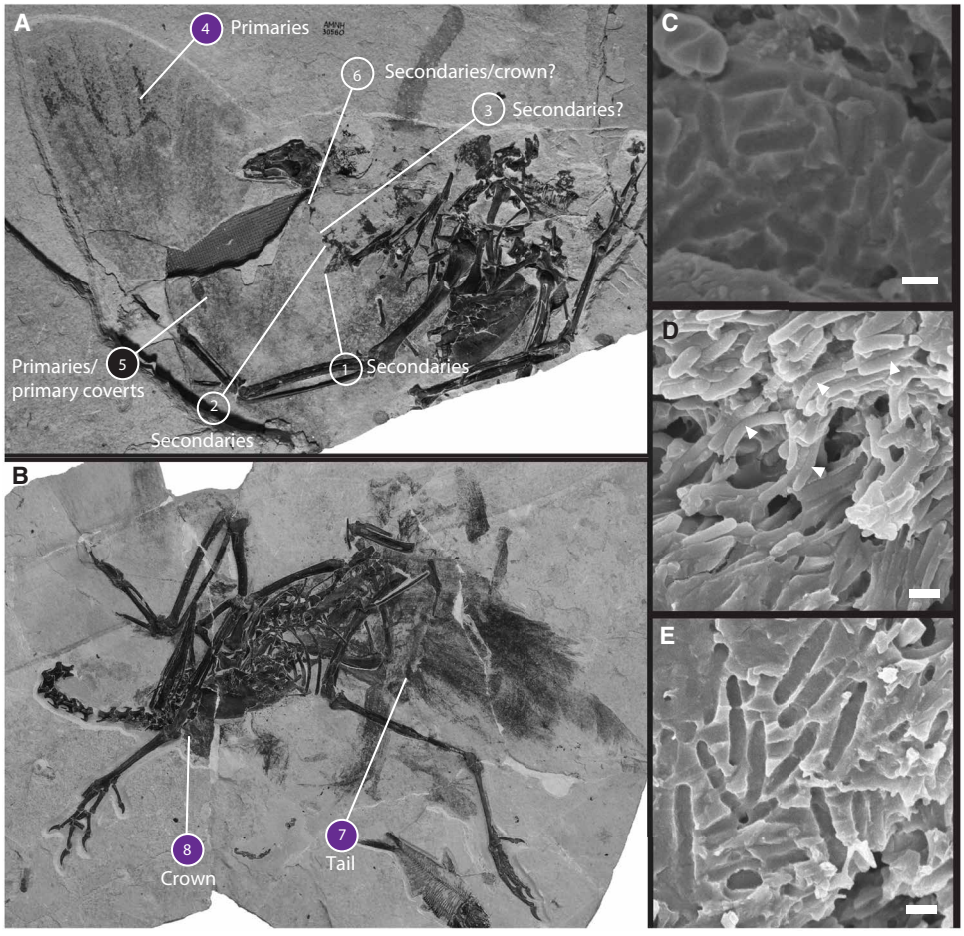

Fig. 2. Sampling map of two Lithornithid fossils from the Green River Formation in Wyoming. Lithornithid specimens AMNH FARB 30578 (**A**) and AMNH FARB 30560 (**B**) used with permission from Nesbitt and Clarke (*15*). Circle color indicates samples predicted as black (black), iridescent (purple), or unknown due to a lack of melanosomes in the sample (unfilled circles). All feather identities are tentative given the disarticulated nature of the specimen, with the exception of some wing and tail remiges. Panels on the right show fossil melanosomes similar to black (sample 5) (**C**) and iridescent melanosome morphologies in extant birds (samples 7 and 8) (**D** and **E**). Scale bars, 500 nm (C to E).

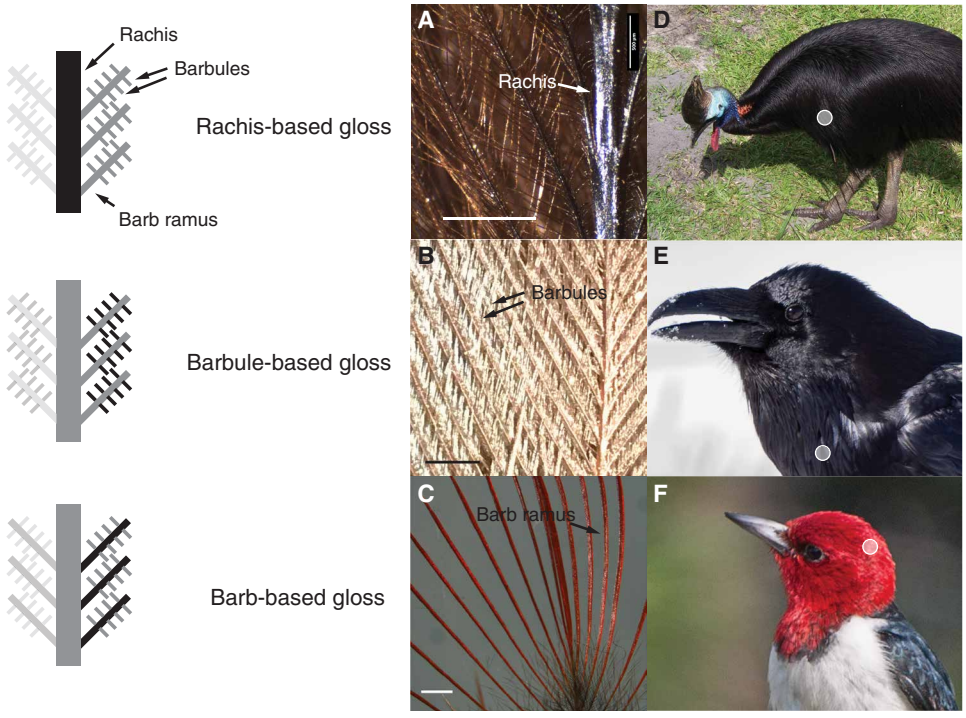

Fig. 3. Diverse mechanisms of gloss production in birds. Feather cartoons depict the anatomical location of structural gloss production (regions shaded in black) in a feather. Gloss can be produced in the feather rachis (**A**, this study), barbules (**B**), or barb rami (**C**). Photos depict feather microstructures responsible for gloss production (A to C) and representative images of a southern cassowary (**D**), common raven (**E**), and red-headed woodpecker (**F**) displaying glossy plumage. Scale bars, 1 mm (A to C). Photo credits: Branislav Igic (C), Scott Hamlin (D), Charles Peterson (E), and Mike Carlo (F).

from the mechanisms in other birds (Fig. 3). Previously known mechanisms of structural gloss production in birds include a thin layer of melanosomes forming a keratin film in feather barbules (*2*) and flattening of feather barbs (*3*). Both of these mechanisms involved production of flat, optical interfaces for reflecting light in a single direction. Kulp *et al.* (*5*) found that gentoo penguins produce gloss in nonpigmented, white feathers and suggested that this might be the result of differences in the smoothness of the feather surface. Our results show an additional source of gloss production in bird feathers: the morphology of the feather rachis. At a mechanistic level, narrow feathers with large, bare rachises (i.e., lacking barbules) reflect more light directionally to increase specular reflectance (fig. S8B), and feathers containing primarily disorganized, moderately elongate melanosomes associated with darker eumelanin pigments (*17*) decrease diffuse reflectance (fig. S8A). This novel rachidial mechanism of gloss production demonstrates functional convergence of glossy feathers (Fig. 3) and highlights the need to consider the physicochemical underpinnings of how glossy signals are produced rather than focusing only on the signals themselves.

As is the case with many complex traits (*18*), the acquisition of traits involved in the exceptional gloss of cassowaries (fig. S3) occurs at different time points rather than evolving all at once. Narrow feather vanes are present in moas (the sister clade of tinamous) (*19*), emus, cassowaries, and kiwis (*12*), suggesting either a single gain in non-rhea/ostrich palaeognaths or a gain in the common ancestor of kiwis, emus, and cassowaries (Fig. 4). Loss of distal feather barbules occurs at different time points, in the cassowary-emu ancestor, while a thickened feather rachis appears to be unique to cassowaries (Fig. 4). The black rachises of their extant sister taxon, emus, closely approach the cassowary condition. However, all ratites show an allometric constraint on melanosome shape (i.e., toward shorter, low aspect ratio melanosomes) linked to lower basal metabolic rates of large-bodied ratites (*20*, *21*). Thus, although elongate melanosomes may facilitate self-assembly into iridescent arrays (*22*), this mechanism appears to not be available as a strategy for structural coloration in any ratites, including cassowaries. Instead, cassowaries produce black structural gloss primarily through feather shape modifications more similar to changes in hair shape and structure observed in some mammals with scale-like body coverings. Theoretically, if a bird were covered in a solid sheet of keratin it would increase gloss even more, thus widespread use of mechanism of gloss in Aves is a constraint of having primarily branched, hierarchical integumentary structures (i.e., feathers).

Lithornithids, extinct, small-bodied Eocene palaeognaths, are found to represent an additional origin of glossy or weakly iridescent black conferred by organized, elongate melanosome arrays (Fig. 2). Morphological innovations behind these arrays have been described in several neognaths, ranging from square arrays of melanosomes in peafowl to hexagonal melanosome configurations in ducks (*13*). Several fossil lineages have also been also inferred on the basis of melanosome morphologies to have glossy or iridescent feathers, including the basal paravian dinosaur *Caihong* (*7*), several Enantiornithes (*23*, *24*), *Microraptor* (*23*), and an Eocene bird (*17*). The phylogenetic placement of lithornithids remains uncertain (*15*). However, using a well-supported molecular phylogeny of crown Paleognathae as a constraint tree, Nesbitt and Clarke (*15*) recovered lithornithids at the base of the palaeognath total group, outside the crown (Fig. 4); without these constraints, analyses recover them as the sister taxon

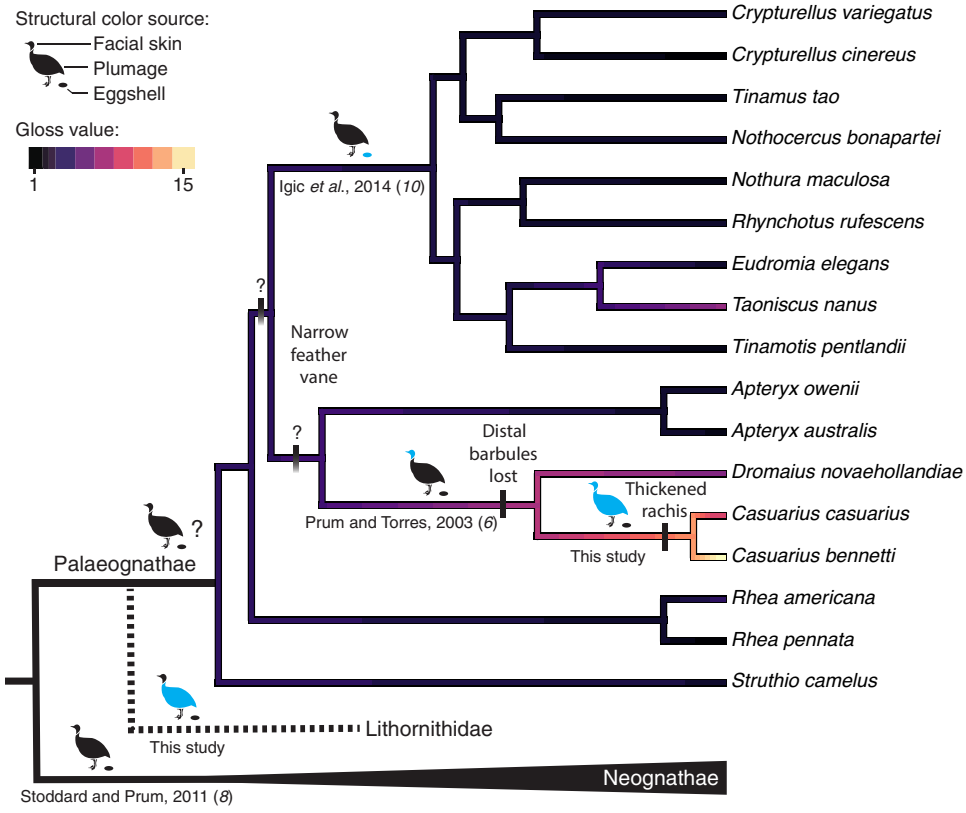

Fig. 4. Structural color evolution in palaeognaths. Cartoon birds depict evolutionary origins of structural coloration in eggshells, feathers, and skin (blue body regions). Branches show estimated ancestral states of glossiness based on reflectance data (see legend). A Bayesian model involving a discrete "jump" in glossiness within the cassowary and emu clade received the strongest support (posterior probability of a shift occurring in this clade, >0.5; see Materials and Methods and fig. S3). Loss of barbules and thickened rachises (vertical dashes; see figs. S6 and S7 for full results) in the cassowary-emu clade may contribute to this pattern. Uncertainty in the origin of a narrow feather vane is indicated with shaded boxes and questions marks. Placement of Lithornithidae based on parsimony analysis of Nesbitt and Clarke (*15*) using a constraint tree based on molecular data (*33*).

to tinamous (*15*). Whether the capability for structural color production via organization of elongate melanosome shapes in barbs evolved only in lithornithids (Fig. 2) or whether it was present in the ancestral palaeognath and then lost, the new data support the presence of the developmental toolkit to produce elongate melanosomes as ancestral to a much more inclusive clade, Paraves.

While environment and other aspects of ecology may influence selection on ornaments generally, integument structure and metabolism may also limit available strategies for generating particular kinds of ornaments such as a glossy integument. Evidence of melanosome morphologies associated with glossy and iridescent colors in the feather barbules of neognath birds (*2*) are so far not known in the hairs of mammals, filaments of dinosaurs and pterosaurs, or rachises of extant palaeognath and neognath birds. One exception may be golden moles that produce structural color with novel a multilayered structure in their hairs (*25*). We find evidence for a novel mechanism of bright gloss, most similar to that in mammalian hair, in a flightless bird with no distal feather barbules and reduced barbs. The diversity of mechanisms for melanin-based structural colors may thus be limited by the type of integument structure, for example, with distinct strategies for similar colors in filaments and pinnate feathers. Prior work suggests that shifts in the melanocortin system associated with lower metabolic rates in large-bodied avian taxa may additionally constrain the evolvability of certain color mechanisms (*9*, *21*). Further investigation of these hypotheses may be the key to understanding vertebrate coloration more generally. Differences in the parts of the feather generating the structural color or gloss—the rachis in the case of cassowaries compared to feather barbules in other glossy black neognath birds (*2*)—should result in major differences in genic and regulatory targets of selection. Several genes that have been identified as involved in explaining rachis diameter, including growth differentiation factor 10 (GDF10) and bone morphogenetic protein 2 (BMP2) (*26*), may be key foci for further work in this area. Integration developmental, anatomical, and paleontological evidence may inform potential constraints and trade-offs in the evolution of integumentary structures and coloration mechanisms.

MATERIALS AND METHODS

Spectrophotometry

To quantify gloss, we measured both specular and diffuse reflectance for 32 feathers from 17 species of palaeognaths, including eight flightless ratites and nine tinamous. Feathers were sampled at the Harvard Museum of Comparative Zoology (MCZ), the Zoological Museum Amsterdam, the National Museum of Natural History (RMNH), and the University of Texas at Austin Vertebrate Paleontology Lab (UTVPL) (see dataset S1). Specular reflectance was measured with the light and detector both at an angle of 60° from the perpendicular

to the feather surface, using an Avantes AvaSpec-2048 spectrometer with an AvaLight-XE pulsed xenon light source with an integration time of 100 ms and averaging 10 scans. We took three spectra, moving the reflectance probe 1 to 2 mm between readings to ensure that we averaged over the visible feather area. Diffuse reflectance was measured with an integrating sphere (AvaSphere-50-REFL, Avantes), taking the average of two scans at an integration time of 4000 ms. We calculated the average specular and diffuse reflectance over 300- to 700-nm wavelengths and Hunter's contrast gloss (*27*) as the average of the ratio between specular and diffuse reflectance values (fig. S1).

Feather imaging

To examine whether the surfaces of cassowary feathers were smoother than our negative controls, we imaged the feather surface using an AIST-NT SmartSPM 1000 AFM. We compared nanoscale surface roughness of the southern cassowary (*Casuarius casuarius*, UTVPL M-12033) to negative controls with matte feathers: common ostrich (*Struthio camelus*, RMNH 5843) and gray tinamou (*Tinamus tao*, MCZ 173014). To quantify surface roughness, we identified a ~4-μm × 4-μm region of interest (ROI) for the rachis and barb ramus of one feather sample per species in the program Gwyddion v. 2.50. We then masked irregularities (e.g., dirt on the feather surface) using the rectangular masking tool, leveled the three-dimensional contour using mean plane subtraction, and calculated root mean square roughness of each unmasked ROI per feather sample. We additionally used a FEI Tecnai TEM (Tecnai, Hillsboro, OR) to examine whether cassowary feathers have nanostructural features previously shown to be involved in gloss production in neognaths, such as melanosome arrangement and the presence of a thin keratin cortex at the surface of feather barbules (*2*).

Quantifying feather morphology

We used a Leica EZ4D dissecting microscope to image feather microstructure. We then measured the following traits in ImageJ: (i) vane width at the midpoint along the length of the feather, (ii) feather length from base to tip of the rachis, (iii) rachis diameter at the midpoint of the feather, and (iv) the presence of barbules at the distal end of the feather (see dataset S1). Because overall feather size can vary depending on the body region sampled, we also calculated relative rachis diameter by dividing rachis diameter by vane width. We combined these data with measurements of (v) melanosome density and (vi) melanosome length from a published melanosome dataset (*9*).

Fossil melanosomes

Using two published datasets on melanosome morphologies in crown birds and nonavian dinosaur taxa (*7*, *16*), we performed a quadratic discriminant function analysis to predict color in an extinct lithornithid, *C. grandei* (*15*). We examined two specimens: AMNH FARB 30578 (the holotype) and AMNH FARB 30560. Both specimens are from the Early Eocene Green River Formation, with an estimated age of 51.66 ± 0.09 million years (*15*). To assess melanosome morphology, we removed small ~1-mm flakes at locations in the slab where feathers were visible but covered by unprepared matrix, removing the counterpart to the mostly exposed feather. We then placed the samples on SEM stubs and sputter-coated them with palladium/platinum on a Cressington 208 Sputter Coater. We used a Zeiss Supra 40VP SEM to image fossilized melanosomes and lastly measured the length and width of between 10 and 113 individual melanosomes per sample (Table 2) using ImageJ (*28*) and following established protocols (*7*).

Comparative analyses

Identifying evolutionary shifts in glossiness

To assess whether cassowaries are exceptionally glossy relative to other palaeognaths, we used a Bayesian method implemented in the R package bayou (*29*) to calculate the location of shifts in the evolutionary mean of a trait. We used half-Cauchy priors for the restraining parameter (α) and rate of evolution (σ^2), along with a normal prior for the ancestral state (θ) (*29*). To avoid spurious results (e.g., nonreplicated regime shifts owing to longer terminal branches relative to internodes), we only allowed shifts to be estimated on nonterminal branches. We ran the Markov chain Monte Carlo (MCMC) chain for 10^6 generations, sampling every 10^3 generations and discarding 25% of the samples as burn-in. Given the small sample sizes (17 species), we tested the sensitivity of the recovered evolutionary shifts using the l1ou R package (*30*). This method simulates evolution for a given set of parameters (e.g., evolutionary rate σ^2 and restraining parameter α) and estimates the percentage of times the simulated datasets recover the same node shifts as the empirical dataset. This analysis showed that the bayou-estimated shifts within emus and cassowaries are recovered 90% of the time for the simulated datasets (fig. S3).

Phylogenetic regressions

To understand the relationship between feather morphology and reflectance parameters (specular, diffuse reflectance), we used PLMMs in the MCMCglmm R package (*31*). To our knowledge, this is the only method that can account for within-species sampling (e.g., four distinct feathers sampled from *Crypturellus variegatus*; fig. S1 and dataset S1) at the same time as accounting for potential trait covariation owing to the shared evolutionary history of species. Our model included specular and diffuse reflectance as a response and melanosome aspect ratio, melanosome density, presence of barbules, and proportional rachis diameter as predictors. Melanosomes were not found in one species with white plumage (*Eudromia elegans*), thus we removed this species from our statistical analyses. We ran MCMC chains for 10^6 generations, sampling every 1000 generations and discarding 25% of the posterior samples as burn-in. We checked the output using trace plots. We compared two models using the deviance information criterion (DIC): (i) a Brownian motion model of trait evolution and (ii) a "white noise" model in which species relationships do not explain the observed trait variation. In most cases, the Brownian motion model was preferred (see table S1 for DIC weights), and we only discuss results of the preferred models further.

Covariance analysis of spectral data

To determine whether the relationship between specular and diffuse reflectance differs between the focal clade (cassowaries and emus) and "background" palaeognaths, we used a Bayesian approach to estimate phenotypic covariance structure (*32*). Briefly, we fit a model in MCMCglmm allowing for different covariance between these groups (see Dryad for R code). We ran the MCMC chain for 10^6 generations, with a burn-in of 25% and a sampling interval of 1000 generations. We then determined whether the angle of maximum variation (g_{max} or the slope) between specular and diffuse reflectance differed among groups by computing the angles between and among groups for all posterior samples from the MCMC analysis. We determined significance as the proportion of simulations in which

the between-group divergence in g_{max} was greater than the within-group divergence (*32*).

SUPPLEMENTARY MATERIALS

Supplementary material for this article is available at http://advances.sciencemag.org/cgi/content/full/6/20/eaba0187/DC1

View/request a protocol for this paper from *Bio-protocol*.

REFERENCES AND NOTES

1. R. O. Prum, Anatomy, physics, and evolution of avian structural colors, in *Bird Coloration*, K. J. Mcgraw, G. E. Hill, Eds. (Harvard Univ. Press, 2006), vol. 1, pp. 295–353.
2. R. Maia, L. D'Alba, M. D. Shawkey, What makes a feather shine? A nanostructural basis for glossy black colours in feathers. *Proc. R. Soc. B* **278**, 1973–1980 (2010).
3. J.-P. Iskandar, C. M. Eliason, T. Astrop, B. Igic, R. Maia, M. D. Shawkey, Morphological basis of glossy red plumage colours. *Biol. J. Linn. Soc.* **119**, 477–487 (2016).
4. L. D'Alba, V. Saranathan, J. A. Clarke, J. A. Vinther, R. O. Prum, M. D. Shawkey, Colour-producing β-keratin nanofibres in blue penguin (*Eudyptula minor*) feathers. *Biol. Lett.* **7**, 543–546 (2011).
5. F. B. Kulp, L. D'Alba, M. D. Shawkey, J. A. Clarke, Keratin nanofiber distribution and feather microstructure in penguins. *Auk* **135**, 777–787 (2018).
6. R. O. Prum, R. Torres, Structural colouration of avian skin: Convergent evolution of coherently scattering dermal collagen arrays. *J. Exp. Biol.* **206**, 2409–2429 (2003).
7. D. Hu, J. A. Clarke, C. M. Eliason, R. Qiu, Q. Li, M. D. Shawkey, C. Zhao, L. D'Alba, J. Jiang, X. Xu, A bony-crested Jurassic dinosaur with evidence of iridescent plumage highlights complexity in early paravian evolution. *Nat. Commun.* **9**, 217 (2018).
8. M. C. Stoddard, R. O. Prum, How colorful are birds? Evolution of the avian plumage color gamut. *Behav. Ecol.* **22**, 1042–1052 (2011).
9. C. M. Eliason, M. D. Shawkey, J. A. Clarke, Evolutionary shifts in the melanin-based color system of birds. *Evolution* **70**, 445–455 (2016).
10. B. Igic, D. Fecheyr-Lippens, M. Xiao, A. Chan, D. Hanley, P. R. L. Brennan, T. Grim, G. I. N. Waterhouse, M. E. Hauber, M. D. Shawkey, A nanostructural basis for gloss of avian eggshells. *J. R. Soc. Interface* **12**, 20141210 (2014).
11. W. Rothschild, W. P. Pycraft, A monograph of the genus casuarius. *Trans. Zool. Soc. Lond.* **15**, 109–148 (1900).
12. A. C. Chandler, *A study of the Structure of Feathers: With Reference to Their Taxonomic Significance* (University of California Press, 1916), vol. 13.
13. H. Durrer, Schillerfarben der vogelfeder als evolutionsproblem. *Denkschr. Schweiz. Naturf. Ges.* **91**, 1–127 (1977).
14. H. You, L. Yu, Atomic force microscopy as a tool for study of human hair. *Scanning* **19**, 431–437 (1997).
15. S. J. Nesbitt, J. A. Clarke, The anatomy and taxonomy of the exquisitely preserved green river formation (Early Eocene) lithornithids (Aves) and the relationships of lithornithidae. *Bull. Am. Museum Nat. History* **406**, 1–91 (2016).
16. K. K. Nordén, J. W. Faber, F. Babarović, T. L. Stubbs, T. Selly, J. D. Schiffbauer, P. Peharec Štefanić, G. Mayr, F. M. Smithwick, J. Vinther, Melanosome diversity and convergence in the evolution of iridescent avian feathers—Implications for paleocolor reconstruction. *Evolution* **73**, 15–27 (2019).
17. J. Vinther, D. E. G. Briggs, J. Clarke, G. Mayr, R. O. Prum, Structural coloration in a fossil feather. *Biol. Lett.* **6**, 128–131 (2009).
18. A. Monteiro, O. Podlaha, Wings, horns, and butterfly eyespots: How do complex traits evolve? *PLOS Biol.* **7**, e1000037 (2009).
19. N. J. Rawlence, J. R. Wood, K. N. Armstrong, A. Cooper, DNA content and distribution in ancient feathers and potential to reconstruct the plumage of extinct avian taxa. *Proc. R. Soc. B* **276**, 3395–3402 (2009).
20. S. K. Maloney, Thermoregulation in ratites: A review. *Aust. J. Exp. Agric.* **48**, 1293–1301 (2008).
21. C. M. Eliason, J. A. Clarke, Metabolic physiology explains macroevolutionary trends in the melanic colour system across amniotes. *Proc. R. Soc. B* **285**, 20182014 (2018).
22. R. Maia, R. H. F. Macedo, M. D. Shawkey, Nanostructural self-assembly of iridescent feather barbules through depletion attraction of melanosomes during keratinization. *J. R. Soc. Interface* **9**, 734–743 (2011).
23. Q. Li, K.-Q. Gao, Q. Meng, J. A. Clarke, M. D. Shawkey, L. D'Alba, R. Pei, M. Ellison, M. A. Norell, J. Vinther, Reconstruction of Microraptor and the evolution of iridescent plumage. *Science* **335**, 1215–1219 (2012).
24. J. A. Peteya, J. A. Clarke, Q. Li, K.-Q. Gao, M. D. Shawkey, The plumage and colouration of an enantiornithine bird from the early cretaceous of china. *Palaeontology* **60**, 55–71 (2017).
25. H. K. Snyder, R. Maia, L. D'Alba, A. J. Shultz, K. M. C. Rowe, K. C. Rowe, M. D. Shawkey, Iridescent colour production in hairs of blind golden moles (Chrysochloridae). *Biol. Lett.* **8**, 393–396 (2012).
26. A. Li, S. Figueroa, T.-X. Jiang, P. Wu, R. Widelitz, Q. Nie, C.-M. Chuong, Diverse feather shape evolution enabled by coupling anisotropic signalling modules with self-organizing branching programme. *Nat. Commun.* **8**, ncommc14139 (2017).
27. R. S. Hunter, Methods of determining gloss. *J. Res. Natl. Bur. Stand.* **18**, 19–39 (1937).
28. M. D. Abràmoff, P. J. Magalhães, S. J. Ram, Image processing with ImageJ. *Biophotonics Int.* **11**, 36–42 (2004).
29. J. C. Uyeda, L. J. Harmon, A novel bayesian method for inferring and interpreting the dynamics of adaptive landscapes from phylogenetic comparative data. *Syst. Biol.* **63**, 902–918 (2014).
30. M. Khabbazian, R. Kriebel, K. Rohe, C. Ané, Fast and accurate detection of evolutionary shifts in Ornstein-Uhlenbeck models. *Methods Ecol. Evol.* **7**, 811–824 (2016).
31. J. D. Hadfield, S. Nakagawa, General quantitative genetic methods for comparative biology: Phylogenies, taxonomies and multi-trait models for continuous and categorical characters. *J. Evol. Biol.* **23**, 494–508 (2010).
32. M. R. Robinson, A. P. Beckerman, Quantifying multivariate plasticity: Genetic variation in resource acquisition drives plasticity in resource allocation to components of life history. *Ecol. Lett.* **16**, 281–290 (2013).
33. K. J. Mitchell, B. Llamas, J. Soubrier, N. J. Rawlence, T. H. Worthy, J. Wood, M. S. Y. Lee, A. Cooper, Ancient DNA reveals elephant birds and kiwi are sister taxa and clarifies ratite bird evolution. *Science* **344**, 898–900 (2014).

Acknowledgments: We thank J. Trimble (Harvard Museum of Comparative Zoology), P. Kamminga and R. Desjardins (Naturalis, Leiden), and K. Bader (University of Texas, Vertebrate Paleontology Laboratory) for help with locating and sampling specimens. Z. Li and S. Davis made insightful comments on earlier versions of this manuscript and assisted with feather imaging (S. Davis). **Funding:** We gratefully acknowledge funding from the NSF (NSF EAR 1355292 and NSF EAR 1251922 to J.A.C.). **Author contributions:** J.A.C. and C.M.E. conceived the study, collected and conducted the analyses of data, and wrote the manuscript. **Competing interests:** The authors declare that they have no competing interests. **Data and materials availability:** All datasets and R code used in these analyses are available at Dryad (https://doi.org/10.5061/dryad.8w9ghx3hn). All other data needed to evaluate the conclusions in the paper are present in the paper and/or the Supplementary Materials. Additional data related to this paper may be requested from the authors.

Submitted 28 October 2019
Accepted 13 February 2020
Published 13 May 2020
10.1126/sciadv.aba0187

Citation: C. M. Eliason, J. A. Clarke, Cassowary gloss and a novel form of structural color in birds. *Sci. Adv.* **6**, eaba0187 (2020).

ScienceAdvances

Cassowary gloss and a novel form of structural color in birds

Chad M. EliasonJulia A. Clarke

Sci. Adv., 6 (20), eaba0187.

Science Advances (ISSN 2375-2548) is published by the American Association for the Advancement of Science. 1200 New York Avenue NW, Washington, DC 20005. The title *Science Advances* is a registered trademark of AAAS.